Size-dependent intracellular immunotargeting of therapeutic cargoes into endothelial cells

Rainer Wiewrodt, Anu P. Thomas, Luca Cipelletti, Melpo Christofidou-Solomidou, David A. Weitz, Sheldon I. Feinstein, David Schaffer, Steven M. Albelda, Michael Koval, and Vladimir R. Muzykantov

Cell-selective intracellular targeting is a key element of more specific and safe enzyme, toxin, and gene therapies. Endothelium poorly internalizes certain candidate carriers for vascular immunotargeting, such as antibodies to platelet endothelial cell adhesion molecule 1 (PECAM–1). Conjugation of poorly internalizable antibodies with streptavidin (SA) facilitates the intracellular uptake. Although both small and large (100-nm versus 1000-nm diameter) anti-PECAM/SA–beta galactosidase (SA–β-gal) conjugates bound selectively to PECAM-expressing cells, only small conjugates showed intracellular accumulation of active β-gal. To study whether size of the conjugates controls the uptake, a series of anti-PECAM/SA and anti-PECAM/bead conjugates ranging from 80 nm to 5 μm in diameter were produced. Human umbilical vein endothelial cells and PECAM-transfected mesothelioma cells internalized 80- to 350-nm anti-PECAM conjugates, but not conjugates larger than 500 nm. Further, size controls intracellular targeting of active therapeutic cargoes in vitro and in vivo. Small anti-PECAM/DNA conjugates transfected target cells in culture 5-fold more effectively than their large counterpart (350- versus 4200-nm diameter). To evaluate the practical significance of the size-controlled subcellular addressing, we coupled glucose oxidase (GOX) to anti-PECAM and antithrombomodulin. Both types of conjugates had equally high pulmonary uptake after intravenous injection in mice, yet only small (200- to 250-nm), not large (600- to 700-nm), GOX conjugates caused profound oxidative vascular injury in the lungs, presumably owing to intracellular generation of H_2O_2. Thus, engineering of affinity carriers of specific size permits intracellular delivery of active cargoes to endothelium in vitro and in vivo, a paradigm useful for the targeting of drugs, genes, and toxins. (Blood. 2002;99:912-922)

Introduction

Targeted intracellular drug delivery needed for more effective and safe therapies requires both cell-specific recognition and subsequent internalization. Many internalizable determinants (eg, transferrin receptor) do not enable cell-specific recognition.[1-3] Immunotargeting permits more specific targeting,[4-7] but many antibodies (even some antibodies against internalizable antigens, eg, thrombomodulin [TM]) are poorly internalized.[8-10] Antibody polymerization, coupling with internalizable entities (eg, transferrin or urokinase), and other strategies have been explored to facilitate internalization.[11-13]

Constraints for intracellular delivery depend on cell type and the nature of a target antigen. Among other cells, vascular endothelium is an important target. Stably and highly expressed endothelial antigens, such as platelet endothelial cell adhesion molecule 1 (PECAM–1) or CD31 (a glycoprotein involved in transmigration of leukocytes)[14-18] and TM (CD 141, a glycoprotein controlling enzymatic activities of thrombin),[19] may be used as target determinants, since their blood levels are several orders of magnitude lower than in endothelial cells.[20-22] In addition to the targeting function, anti-PECAM may suppress inflammation.[23-25] Recent studies showed that monoclonal antibodies directed against these determinants (ie, anti-PECAM and anti-TM) could be used for immunotargeting to endothelial cells in vitro and in vivo.[26-29]

Although endothelial cells poorly internalize anti-PECAM, anti-PECAM conjugated with streptavidin (SA) is readily internalized.[28] Both anti-PECAM/SA and anti-TM/SA serve as a carrier to deliver active enzymes and genes to pulmonary endothelial cells in intact animals.[26-32] However, the carrier properties optimal for intracellular targeting to endothelium have not been established.

Conceivably, carrier size is an important parameter for the intracellular uptake, yet this issue has not been systematically addressed in the literature. Available data show that optimal particle size threshold for intracellular uptake varies in different cell types.[7,12,33-36] Although macrophages internalize large complexes of 1 μm in diameter or larger,[37-39] little is known about how the size of complexes affects their uptake by other cell types. There

From the Pulmonary Critical Care Division, Department of Medicine; the Institute for Environmental Medicine; and the Departments of Physiology and Pharmacology, University of Pennsylvania School of Medicine, Philadelphia; the Department of Physics, University of Pennsylvania, Philadelphia; and the Department of Chemical Engineering, University of California, Berkeley.

Submitted March 16, 2001; accepted September 24, 2001.

R.W. is a postdoctoral fellow of the Mildred Scheel Stiftung für Krebsforschung der Deutschen Krebshilfe e.V. (D/98/02288). Supported by the National American Heart Association (Established Investigator Grant 9640204 [V.R.M.]; grant-in-aid 9950389N [M.K.]; Initial Investigator Grant 00301920 [M.C.S.]); and SDG Grant AHA 0030192 [M.C.S.]; American Arthritis Foundation (M.K. is Hulda Irene Dugan Investigator); National Institutes of Health (SCOR in Acute Lung Injury, National Heart, Lung, and Blood Institute grant HL60290, Project 4, [V.R.M., S.M.A]; grant GM61012 [M.K.]; grant HL-53566 and SCOR 1-P50 [S.I.F.]); and National Aeronautics and Space Administration (grant NAG3-2058 [L.C., D.A.W.]). The dynamic light scattering apparatus was funded with National Science Foundation grants DMR-9631279 and DMR-9704300.

Reprints: Vladimir R. Muzykantov (drug delivery and vascular immunotargeting) or Michael Koval (cell biology and internalization), Institute of Environmental Medicine, University of Pennsylvania Medical Center, 1 John Morgan Bldg, 36th St and Hamilton Walk, Philadelphia, PA 19104-6068; e-mails: muzykant@mail.med.upenn.edu, mkoval@mail.med.upenn.edu.

The publication costs of this article were defrayed in part by page charge payment. Therefore, and solely to indicate this fact, this article is hereby marked "advertisement" in accordance with 18 U.S.C. section 1734.

are no studies on effects of size on endothelial internalization via constitutive surface adhesion molecules.

The goal of the present study was (1) to determine whether size controls uptake of anti-PECAM conjugates and to define the maximum size threshold for the uptake by endothelial cells and (2) to evaluate whether the size of immunoconjugates directed against endothelial antigens controls their targeting and effect in vivo. We generated diverse anti-PECAM conjugates ranging from 80- to 5000-nm diameter and found that the conjugates smaller than 350 nm were preferentially internalized by human umbilical vein endothelial cells (HUVECs) and model cells expressing recombinant PECAMs, thus permitting intracellular targeting of active cargoes. We also synthesized small (200- to 250-nm) and large (600- to 700-nm) conjugates of glucose oxidase (GOX) (producing H_2O_2 from glucose) with rat antibodies to murine PECAMs and TM. After intravenous (IV) injection in mice, both small and large anti-TM/^{125}iodine (^{125}I)–GOX and anti-PECAM/^{125}I-GOX accumulated in the lungs to a similar extent, yet only small, not large, conjugates caused a profound oxidative injury in the pulmonary vasculature. Thus, size-controlled engineering of affinity carriers allows intracellular immunotargeting of cargoes to endothelial cells via poorly internalizable surface molecules in vitro and in vivo. This important paradigm may be used for the optimal design of cell-selective targeting of therapeutic cargoes, ie, drugs, genes, and immunotoxins.

Materials and methods

Materials

The following antibodies were used: mouse monoclonal antibody (mAb) anti-PECAM mAb 62 (provided by M. Nakada, Centocor, Malvern, PA)[40]; monoclonal antibody against human TM, mAb CTM 1045 (provided by C. Esmon, Oklahoma Medical Research Foundation, Oklahoma City, OK)[8]; rat monoclonal antibody against murine PECAM, mAb 390[28]; rat monoclonal antibody against murine TM, mAb 273-34 (provided by S. Kennel, Oak Ridge National Laboratories, TN)[26,27]; control murine immunoglobulin G (Ig G; Calbiochem, San Diego, CA); and fluorescent goat antimouse antibodies (Jackson ImmunoResearch, West Grove, PA). Unless otherwise specified, reagents were purchased from Sigma (St Louis, MO). The following cell lines were cultured as described previously[8,28]: HUVECs (Clonetics, San Diego, CA); EAhy926 (an immortalized PECAM-expressing transformed cell line provided by C. Edgel, University of North Carolina, Chapel Hill); human mesothelioma (REN) cells transfected with complementary DNA (cDNA) encoding human PECAMs (REN/PECAM cells); and control REN, which do not express PECAM.[28,41,42]

Antibody conjugates: preparation and size determination

Antibodies and IgG were biotinylated with NHS-LC-biotin (Pierce, Rockford, IL) and conjugated with SA (90% unlabeled, 10% rhodamine labeled) as previously described.[4] Under these conditions, we estimate that conjugates larger than 80 nm will include at least one rhodamine SA on average. Biotinylated antibodies were labeled with ^{125}I by means of Iodogen (Pierce). Fluorescent latex beads (Fluoresbrite plain YG microspheres) (Polysciences, Warrington, PA) were coated with antibodies as previously described.[43] The conjugates and antibody/bead preparations were analyzed by dynamic light scattering (DLS) by means of either an ALV-5000/E Multiple Tau-Digital correlator and goniometer (ALV, Langen, Germany) or a BI-90Plus particle-size analyzer with BI-9000AT Digital autocorrelator (Brookhaven Instruments, NY) at a 90° angle. The effective diameter was calculated by means of the Stokes-Einstein relationship from the diffusion coefficient, obtained from a second-order cumulant fit to the data[44]; multiple runs were performed (mean ± SEM).

Binding and internalization of anti-PECAM/SA and anti-PECAM/bead conjugates

To trace the uptake of antiendothelial carriers, HUVECs, EAhy926 cells, or REN/PECAM cells were incubated with ^{125}I-labeled biotinylated anti-PECAM or anti-TM mAbs, or with their SA-conjugated counterparts, for 90 minutes at 37°C. After washing off nonbound materials, the surface-associated radioactivity was eluted by glycine buffer (pH 2.5), while the intracellular radioactivity was determined in cell lysates as described previously.[8,28]

To visualize the uptake of the rhodamine-labeled conjugates, cells plated on glass coverslips were incubated with the conjugates (10 μg/mL in serum-free culture medium 199 for HUVECs; RPMI for REN and REN/PECAM cells). The cells were washed 5 times and fixed for 10 minutes at room temperature (RT) with 2% paraformaldehyde in phosphate-buffered saline (PBS). The nonpermeabilized cells were then counterstained by fluorescein isothiocyanate (FITC)–conjugated goat antimouse IgG. After washing, the cells were mounted onto glass slides with Mowiol 4-88 (Calbiochem) and imaged by fluorescence microscopy. Incubation of cells with antibody/bead complexes was comparable to the procedures described above, except that Texas Red–conjugated goat antimouse IgG was used for counterstaining, since the beads were FITC-labeled.

Image analysis

Fluorescence microscopy was performed with an Olympus IX-70 inverted fluorescence microscope with the use of filters optimized for FITC (excitation BP, 460 to 490 nm; dichroic DM, 505 nm; emission BA, 515 to 550 nm) and for Texas Red (excitation BP, 530 to 550 nm; dichroic DM, 570 nm; emission BA, 590 to 800 nm) (Chroma Technology, Brattleboro, VT). Images were captured with a Hamamatsu Orca-1 CCD camera and Image Pro 3.0 software (Media Cybernetics, Silver Spring, MD). FITC and Texas Red images were separately obtained by means of gain and exposure times that were optimized to produce 8-bit images with average background intensity values of approximately 20 bits per pixel and average maximum intensity values of approximately 250 bits per pixel (below saturation). Once the settings were established, they were used for all images obtained for a given sample. Using single-labeled preparations, we found that the level of bleed-through was at or below background levels. Single-labeled conjugates and beads were taken to be internalized, while double-labeled conjugates and particles were extracellular.

For anti-PECAM/SA, the Texas Red image (T) contained all of the conjugates in the field, while the FITC image (F) showed only extracellular conjugates. For particle quantitation, double-labeled particles were identified by generating a new image as the logical operation T and F, which was then scored automatically with the constraint that only regions with 4 or more continuous pixels and with an intensity threshold of 128 were counted as extracellular particles. The Texas Red image was then scored in a compatible manner to give the total number of particles in the field; then the fraction of extracellular conjugates for the field was calculated. For antibody/bead complexes, the analysis was comparable, except that the FITC image contained all of the beads and the Texas Red channel showed only extracellular complexes. In some experiments, we calculated the total number of antibody/bead complexes per cell by a similar methodology. Calculations were based on at least 5 fields per experimental treatment and expressed as the mean ± SEM of determinations from multiple experiments. Statistical significance was determined by means of the Student *t* test.

Preparation and characterization of anti-PECAM/SA–β-galactosidase conjugates

The molar ratios of SA–β-galactosidase (SA–β-gal) to biotinylated proteins varied from 0.25 to 1.5 to obtain conjugates with different sizes. The mean diameter of the small anti-PECAM/SA–β-gal was 121 ± 12 nm, while that of the large conjugate was 1183 ± 199 nm (according to 90° DLS). Both conjugates showed full enzymatic activity. REN/PECAM cells were incubated with anti-PECAM/SA–β-gal (10 μg SA–β-gal per well, 24-well plate) for 1 hour at 37°C. After washing of the nonbound conjugates, β-gal enzyme activity in the conjugate preparations and cell lysates was

determined by means of a β-gal enzyme assay kit (Promega, Madison, WI). The β-gal assay activity was normalized according to protein content (BCA Protein Assay Kit) (Pierce). Cells in the parallel wells were stained with X-gal (GibcoBRL, Grand Island, NY).

Studies of radiolabeled anti-PECAM/avidin/DNA complexes

Plasmid DNA from pEGFP-C1 (Clontech, Palo Alto, CA) was digested with Eco RI, then dephosphorylated by means of shrimp alkaline phosphatase (Amersham Pharmacia Biotech, Piscataway, NJ) and labeled with γ-^{32}P–deoxyadenosine triphosphate (3000 Ci/mmol [1.1 × 10^{14} Bq]) by means of polynucleotide kinase (New England Biolabs, Beverly MA). Unreacted nucleotides were removed by gel filtration, and the labeled plasmid DNA was religated by means of T4 DNA ligase (New England Biolabs). The stability of the label was tested in the religated plasmid by subjecting it to digestion with shrimp alkaline phosphatase. The labeled, ligated plasmid was complexed with avidin by incubation for 1 hour at 4°C. To test the antigen-binding properties of anti-PECAM/avidin/DNA complex, plastic wells were coated with purified PECAM-1 and blocked with albumin as described previously.[28] The complexes were incubated in the wells for 1 hour at RT, and after elimination washing, the radioactivity in the wells was determined in a beta counter. Anti-PECAM/avidin/DNA complex was also incubated with HUVECs, REN/PECAMs, or control REN cells for 90 minutes at 37°C, and after washing, the cells were lysed and radioactivity in the wells was determined in a beta counter.

Rhodamine-labeled anti-PECAM/polylysine-SA/cDNA complex studies

To test functional activity of the conjugated DNA, we used a plasmid encoding green fluorescent protein (GFP; pEGFP-C1) (Clontech) and a rhodamine-labeled GFP (rhod-GFP) (Gene Therapy Systems, San Diego, CA). The DNA polyplex consists of molecules of biotinylated anti–PECAM-1 or biotinylated IgG coupled to the plasmid via SA bridges. Poly-L-lysine (181 lysine residues) and SA were chemically cross-linked with N-succinimidyl 3-[2-pyridyldithio]proprionate as previously described.[35] Per 1 μg DNA, 1.5 μg SA-polylysine (electroneutral with DNA) was incubated on ice for 10 minutes, and then 6 μg antibody was added. Polyplex synthesis in 1 M NaCl/20 mM Hepes buffer and 0.1 M NaCl/2 mM Hepes provided smaller (diameter, 350 ± 28 nm) and larger (diameter, 4200 ± 248 nm) polyplexes, respectively. Transfections were performed in REN and REN/PECAM cells in 96-well plates (0.1 μg DNA per well) in physiologic conditions (serum containing medium without chloroquine). As a positive control, nonviral gene transfer was performed with liposomes (Lipofectin, GibcoBRL) with an effective diameter of 230 ± 11 nm. Transgene expression was assessed by means of fluorescent microscopy (number of GFP^+ cells per well) and FACS analysis.

Preparation and administration of GOX conjugates in mice

We produced the trimolecular conjugates b–anti-PECAM/SA/b-GOX (anti-PECAM/GOX); b–anti-TM/SA/b-GOX (anti-TM/GOX); and b-IgG/SA/b-GOX (IgG/GOX) using a 2-step procedure as described.[29,31,45] After SA and b-GOX were mixed and incubated for 1 hour on ice, the complex was then incubated with b–anti-TM, b–anti-PECAM, or b-IgG to form anti-TM/GOX, anti-PECAM/GOX, or their nonimmune counterpart, IgG/GOX. When the molar ratios between SA/b-GOX and biotinylated antibodies were varied, sizes ranged from 100- to 2000-nm diameter, determined by DLS. Enzymatic activity of b-GOX conjugated with carriers did not differ from that of the initial preparation of b-GOX (approximately 100 U/mg).

We characterized the pulmonary targeting of radiolabeled anti-TM/^{125}I-GOX, anti-PECAM/^{125}I-GOX, or IgG/^{125}I-GOX GOX in intact BALBc mice (Charles River Laboratories, NJ) using our established protocol.[29,31] The radioactivity of the dissected internal organs was determined in a gamma counter (Wallac-LKB, Gaithersburg, MD) to calculate the percentage of injected dose per gram of tissue.

To study the effects of GOX immunotargeting, anesthetized mice were killed 4 hours after injection with 50 μg anti-TM/GOX or anti-PECAM/GOX conjugates in saline via tail vein. Our previous study documented that injection of 100 μg IgG/GOX did not cause lung injury.[29,31] Lungs were inspected en bloc to estimate gross injury index by means of the acute lung injury score (ALIS), ranging from 1 (basal level) to 10 (severe hemorrhage and edema), and wet-to-dry ratios were performed as described.[29,31] The lungs allocated for histological studies were processed for conventional paraffin histology. Sections were stained with hematoxylin/eosin and were immunostained for products of lipid peroxidation with a rabbit polyclonal antibody against the isoprostane $iPF_{2\alpha}$-III.[29,31]

Results

Internalization of PECAM- and TM-directed SA conjugates

Glycine elution assay showed that HUVECs, $EAhy_{926}$, and REN/PECAM cells poorly internalized ^{125}I-labeled anti-PECAM mAbs, but SA caused 60% to 90% internalization of biotinylated anti-PECAM mAb 4G6 and mAb 62 (Table 1). SA also facilitated internalization of a poorly internalizable TM monoclonal antibody, mAb CTM 1045, in HUVECs from 20% to 60% (Table 1).

Differential uptake of small and large anti-PECAM/enzyme conjugates by the target cells

We synthesized small (120 nm) and large (greater than 1000 nm) anti-PECAM/SA–β-gal conjugates to examine whether the size controls the intracellular uptake of reporter enzyme conjugates. Both large and small β-gal conjugates bound to the REN/PECAM, but not to REN cells. The total β-gal enzymatic activity recovered in the REN/PECAM cells after 1-hour incubation at 37°C with either large or small conjugates was equivalent (Figure 1A). Our recent study using β-gal immunostaining and confocal microscopy documented that 100- to 200-nm conjugates accumumulate intracellularly in endothelial cells in cell culture and in vivo.[29,31] Small anti-PECAM/SA–β-gal showed a homogenous, intracellular pattern of β-gal activity (Figure 1C). In contrast, the enzymatic activity of large anti-PECAM/SA–β-gal was localized in numerous particles, presumably on the cell surface (Figure 1D).

Table 1. Effect of streptavidin on internalization of platelet endothelial cell adhesion molecules and thrombomodulin antibodies in cell cultures

Cell culture type	$Eahy_{926}$	REN/PECAMs	HUVECs	HUVECs	HUVECs
Antibody	4G6	62	62	4G6	CTM 1045
Antigen	PECAM	PECAM	PECAM	PECAM	TM
No streptavidin	19.2 ± 1.6	22.3 ± 0.5	16.6 ± 6.4	17.9 ± 0.7	20.5 ± 8.3
Plus streptavidin	53.1 ± 1.1	87.9 ± 1.4	79.4 ± 4.2	86.5 ± 1.3	65.3 ± 9.1

$EAhy_{926an}$ is an immortalized platelet endothelial cell adhesion molecule–expressing transformed cell line; REN/PECAMs are human mesothelioma cells transfected with complementary DNA encoding human platelet endothelial cell adhesion molecules; CTM is a monoclonal antibody against human thrombomodulin.

HUVECs indicate human umbilical vein endothelial cells; PECAMs, platelet endothelial cell adhesion molecules; TM indicates thrombomodulin.

The cells were incubated with ^{125}I-labeled biotinylated antibodies ("no streptavidin") or with the streptavidin-conjugated counterparts ("plus streptavidin") for 90 minutes at 37°C. After washing, fractions of cell-surface associated and internalized iodine-125 were determined in glycin eluates and cell lysates. The data are shown as percentage of internalization, mean ± SD; n = 3.

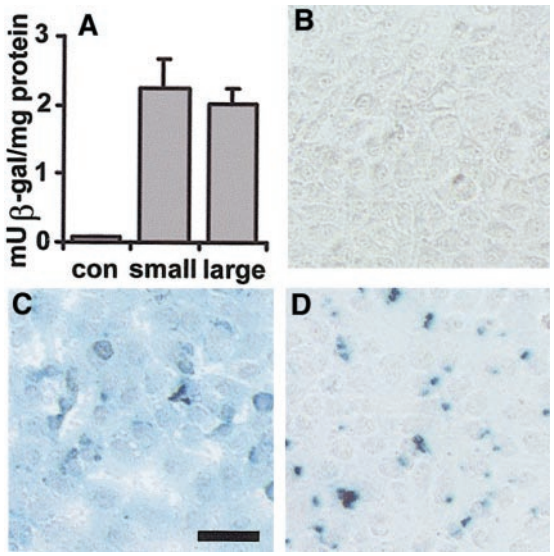

Figure 1. Immunotargeting of small (100 nm) and large (1000 nm) anti-PECAM/SA–β-gal conjugates to REN/PECAM cells. Small and large anti-PECAM/SA (121 ± 12 nm versus 1183 ± 199 nm) and IgG/SA–β-gal (109 ± 12 nm) were incubated with REN/PECAM cells. The β-gal enzyme activity in the conjugate preparations and cell lysates was determined by means of a β-gal enzyme assay kit. Cells were incubated in reporter lysis buffer, then harvested by scraping, and centrifuged. Enzymatic β-gal activity was measured in the supernatants at various dilutions. In the other parallel wells, for X-gal staining, cells were fixed with paraformaldehyde, washed with magnesium chloride, and stained in the dark with a solution containing 1 mg/mL X-gal. Both large and small conjugates delivered equivalent total β-gal enzymatic activity to REN/PECAM cells (A), while control cells incubated with nonimmune counterpart showed no detectable activity (B). Small anti-PECAM/SA–β-gal provided a homogenous intracellular pattern of β-gal activity (C), while large conjugates were associated with a particulate matter apparently localized on the cell surface (D). Bar, 25 μm.

Preferential internalization of small anti-PECAM/SA conjugates by target cells

The above result implied that size controls the uptake of the conjugates. To analyze this issue more precisely, we varied the molar ratio of biotinylated anti-PECAM to rhodamine-labeled SA from 1:2 to 8:1 to form fluorescent anti-PECAM/SA conjugates of diverse size (Figure 2A-E). The conjugate formed at 2-fold excess of b–anti-PECAM was visible by fluorescence microscopy, while other conjugates were difficult to visualize because of the 100-nm resolution limit of the fluorescent microscope. DLS analysis (Figure 2F) confirmed that anti-PECAM/SA prepared at a molar ratio of 2:1 showed the largest size (diameter, 5130 ± 600 nm; n = 5) and revealed that conjugates prepared at a molar ratio of 1:1 and 4:1 had diameters of 221 ± 17 and 174 ± 6 nm (n = 4). Conjugate size diminished at further excess of either component; eg, anti-PECAM/SA prepared at molar ratio of 8:1 had a diameter of 45 nm.

Regardless of size, anti-PECAM/SA, but not IgG/SA, conjugates bound selectively to HUVECs and REN/PECAM cells. We compared internalization of "large" (5130-nm diameter, prepared at a molar ratio 2:1) and "small" (180-nm diameter, prepared at a molar ratio 2:3) anti-PECAM/SA conjugates by HUVECs. Incubation of either large or small conjugates at 4°C did not allow internalization; this was consistent with uptake through an energy-dependent, vesicle-mediated internalization process (not shown). Incubation of the cells with the conjugates at 37°C resulted in the appearance of patches on the apical surface, probably owing to redistribution of the antigen from intercellular borders. Figure 3 shows fluorescent images of HUVECs after incubation with the rhodamine-labeled anti-PECAM/SA conjugates for 60 minutes at 37°C, followed by fixation and staining with FITC-labeled goat antimouse IgG. Cells were not permeabilized; thus, intracellular anti-PECAM/SA appears red, while extracellular double-labeled anti-PECAM/SA appears yellow (typical for large anti-PECAM/SA; Figure 3F). This is perhaps better visualized in the Figure 3 image maps where panels B and F look similar, suggesting that most of the particles were double labeled, while panels A and E do not, suggesting that most of the (small) conjugates in this experiment were not labeled with FITC antibody. Image analysis revealed that 59.7% ± 4.3% (n = 3) of small anti-PECAM/SA was internalized by HUVECs versus 19.6% ± 10.2% (n = 3) of large anti-PECAM/SA (Figure 3G). Similar data indicating preferential internalization of the smaller conjugates were obtained with REN/PECAM cells (not shown).

The size heterogeneity of the large (mean diameter, 5130 nm) anti-PECAM/SA preparation is apparent from fluorescent imaging (Figures 2C, 3F). By a morphometric analysis, we determined which subpopulation of the particles in large anti-PECAM/SA is excluded from the internalization. Fewer than 5% of the intracellular anti-PECAM/SA–containing vesicles in HUVECs were larger than 500 nm. Conversely, more than 75% of the internalized anti-PECAM/SA particles were localized in intracellular vesicles smaller than 250 nm, consistent with the preferential uptake of small anti-PECAM/SA (smaller than 500-nm diameter).

Size threshold for anti-PECAM/bead uptake

We conjugated anti-PECAM to FITC-labeled latex beads ranging from 60 to 480 nm in diameter. Anti-PECAM/beads are inert, are more uniform than anti-PECAM/SA conjugates, have a discrete minimum size threshold (equivalent to the bead diameter), and are stable, permitting us to exclude conjugate degradation as part of the size-separation mechanism. DLS revealed that coating with anti-PECAM or IgG increased the bead size from the initial diameter (Table 2). The amount of anti-PECAM associated with beads ranged from 100 to 7100 molecules per bead as a function of surface area.

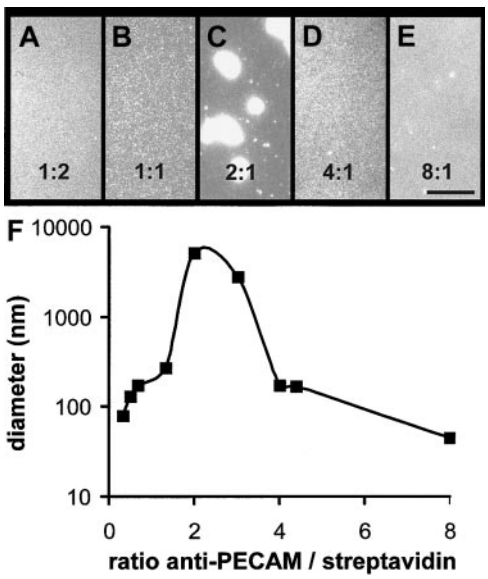

Figure 2. Size of anti-PECAM/SA conjugates. (A-E) Rhodamine-labeled anti-PECAM/SA conjugates were prepared at molar ratios of 1:2 (A), 1:1 (B), 2:1 (C), 4:1 (D), and 8:1 (E) of biotinylated anti–PECAM-1 antibody to rhodamine-SA and were visualized by fluorescence microscopy. Bar, 10 μm. (F) The size of representative anti-PECAM/SA conjugates was determined by DLS and plotted.

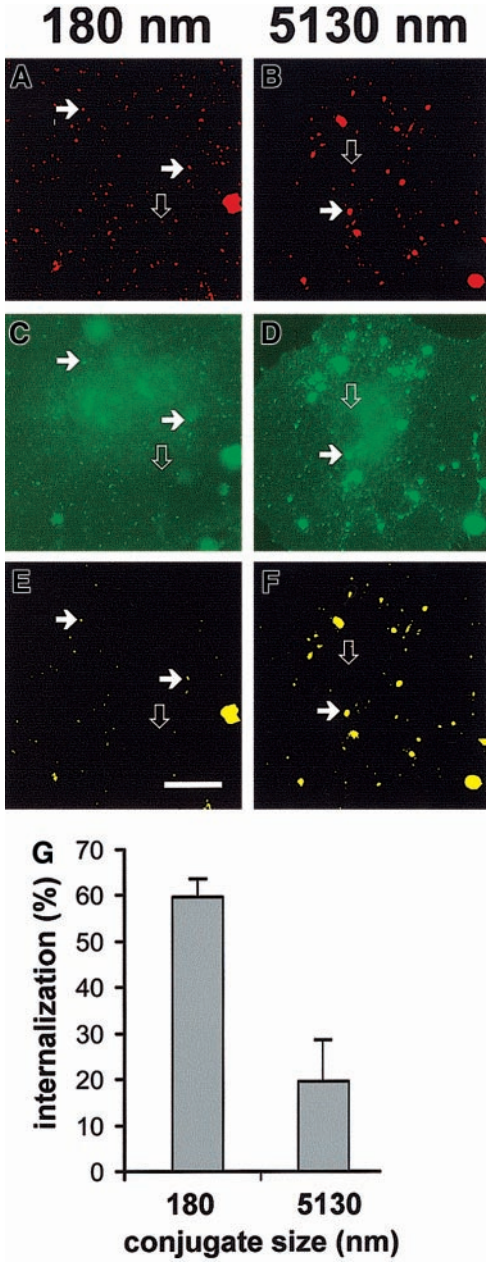

Figure 3. Differential uptake of large and small anti-PECAM/SA conjugates by HUVECs. (A-F) Conjugates were prepared at a molar ratio of anti-PECAM to rhodamine-SA of 2:3 (effective diameter, 180 nm; panels A,C,E) and 2:1 (effective diameter, 5130 nm; panels B,D,F). The conjugates were incubated with HUVECs for 1 hour at 37°C, washed, fixed, and counterstained with FITC-conjugated goat antimouse IgG without permeabilization. The rhodamine channel of fluorescence (C,D) was subjected to a threshold function to eliminate pixels with intensity values lower than 128 to generate an image map of conjugates in the field (A,B). The logical "AND" operation between the conjugate image map (A,B) and the image from the FITC-labeled goat antimouse IgG channel (C,D) were used to generate a colocalization map of noninternalized (yellow) particles (E,F). The solid arrows highlight a noninternalized yellow particle, whereas open arrows indicate internalized conjugates (visible only in the red conjugate image map). Bar, 10 μm. (G) Internalization of small (effective diameter, 180 nm) or large (effective diameter, 5130 nm) conjugates by HUVECs was calculated with the use of the number of noninternalized particles (eg, panels E,F) and total conjugates (eg, panels A,B) as processed above. HUVECs showed roughly 3-fold more internalization of small conjugates than of large conjugates.

Anti-PECAM/beads, but not IgG/beads, bound specifically to HUVECs and REN/PECAM cells (Figure 4). Larger beads (560 nm) possessed almost 2 orders of magnitude more anti-PECAM molecules per bead than smaller beads (130 nm) and could thus engage more PECAM molecules in the cells. To compensate for potential differences in net PECAM cross-linking by small and large anti-PECAM/beads (which may contribute to internalization), we adjusted the number of beads added per cell to attain equivalent amounts of anti-PECAM added per cell (Table 2).

The surface-bound fraction of anti-PECAM/beads was visualized by yellow staining with Texas Red–labeled goat antimouse IgG, whereas intracellular FITC-labeled beads not accessible to the red-antimouse antibody appeared green (Figure 5). Anti-PECAM/beads smaller than 500-nm diameter were readily internalizable: within 1 hour, REN/PECAM cells and HUVECs internalized roughly 50% of cell-associated anti-PECAM/beads ranging from 130 to 310 nm, while 560-nm anti-PECAM/beads showed less than 20% internalization (Figure 5E). Increasing the number of 560-nm anti-PECAM/beads by 10-fold (with about an approximately 30-fold increase of antibody equivalent compared with 130-nm anti-PECAM/beads; Table 2) did not increase the internalization rate (16% ± 4% versus 19% ± 4%, respectively). After 3-hour incubation, 70% to 80% of 130- to 310-nm anti-PECAM/beads were internalized, versus 42% ± 4% of 560-nm anti-PECAM/beads ($P < .01$).

Intracellular delivery of anti-PECAM/SA/DNA and size-dependent transfection of the target cells

To determine whether the size of anti-PECAM carrier affects delivery of DNA, we first coupled ^{32}P-labeled DNA to b–anti-PECAM using a positively charged (isoelectric point, 10.5) avidin that forms stable DNA/avidin complexes capable binding to b-IgG (Figure 6A). Since avidin inhibits the transfection capacity of DNA at ratios higher than 1000 (not shown), we coupled b–anti-PECAM or b-IgG to avidin/^{32}P-DNA complexes formed at a molar ratio of 800:1. Anti-PECAM/avidin/^{32}P-DNA, bound specifically to PECAM-coated plastic wells (Figure 6B) and to HUVECs and REN/PECAM cells (Figure 6C), while IgG/avidin/^{32}P-DNA did not bind to either PECAM-coated wells or PECAM-expressing cells. Thus, the anti-PECAM carrier permits cell-selective delivery of DNA.

To visualize the uptake and transfection in cell cultures, we used a rhodamine-labeled, GFP-encoding cDNA cross-linked to b–anti-PECAM by SA-polylysine[35] (Figure 7). Rhodamine and GFP fluorescence colocalized in REN/PECAM cells incubated with anti-PECAM/SA-polylysine/DNA (350 nm in diameter), yet not all DNA-labeled cells expressed GFP (Figure 7B). Neither rhodamine fluorescence nor GFP expression was detected in the wells with either REN or REN/PECAM cells incubated with IgG/SA-polylysine/DNA conjugate (Figure 7C). Both REN and REN/PECAM cells were equivalently transfected by lipofectin/DNA, while only REN/PECAM cells were transfected with anti-PECAM/SA-polylysine/DNA (Figure 7C). Importantly, small (350-nm) anti-PECAM/SA-polylysine/DNA complexes were approximately 5 times more effective at transfection than the large (4200-nm) complexes (Figure 7D).

Pulmonary immunotargeting and effects of small versus large anti-PECAM/GOX and anti-TM/GOX in intact mice

To study whether the size determines the targeting and effect of the immunoconjugates in vivo, we conjugated the H_2O_2-generating enzyme GOX with antibodies against the murine isoform of PECAM and TM, producing small (200- to 250-nm) and large (600- to 700-nm) anti-PECAM/GOX and anti-TM/GOX conjugates. The specific enzymatic activity of GOX was equal in

Table 2. Properties of anti–platelet endothelial cell adhesion molecule/beads

Uncoated bead size (nm)	Antibody-coated bead size (nm)	Antibody/bead (no. molecules)	Beads added per well ($\times 10^9$)	Antibody equivalent per well ($\times 10^9$)
59 ± 3	128 ± 6	109 ± 8	300	3.3 ± 0.2
100 ± 3	150 ± 8	314 ± 13	100	3.1 ± 0.1
209 ± 10	309 ± 16	1372 ± 93	20	2.7 ± 0.2
477 ± 5	559 ± 23	7148 ± 106	12	8.6 ± 0.1

Specifications for bead size, concentration, and protein-binding capacity are from the manufacturer (Polysciences, Warrington, PA). The IgG-binding capacity of polystyrene latex beads was calculated as previously described.[43] Different amounts of immunobeads were added to the cells in order to attain engagement of a similar number of platelet endothelial cell adhesion molecules per cell. This parameter is calculated as the immunoglobulin-G equivalent per well.

all conjugates (100 mU/mg). Both small and large anti-PECAM/^{125}I-GOX and anti-TM/^{125}I-GOX, but not IgG/^{125}I-GOX, accumulated in the murine lungs after intravenous injection. In fact, the pulmonary uptake of the large anti-TM/GOX conjugate was even higher than that of the small counterpart (Figure 8A). A similar result was obtained with large and small anti-PECAM/^{125}I-GOX conjugates (data not shown). However, injection of 50 μg small, but not large, GOX conjugates caused a profound oxidative vascular injury in the lungs. Within 4 hours, small anti-TM/GOX caused acute lung hemorrhages (Figure 8C), pulmonary vascular congestion, edema and sequestration of white blood cells (Figure 8F), and tissue accumulation of products of lipid peroxidation revealed by immunostaining for iPF$_{2\alpha}$-III, an isoprostane formerly known as 8-epi or 8-isoPGF$_{2\alpha}$ (Figure 8I). In contrast, lungs harvested after injection of large anti-TM/GOX were hardly distinguishable from those harvested from animals in control groups injected with IgG/GOX or PBS (Figure 8B-J). Figure 8K-L also shows parameters of the lung injury after injection of small versus large anti-PECAM/GOX conjugates. In terms of both pulmonary edema determined by lung wet-to-dry ratio and the

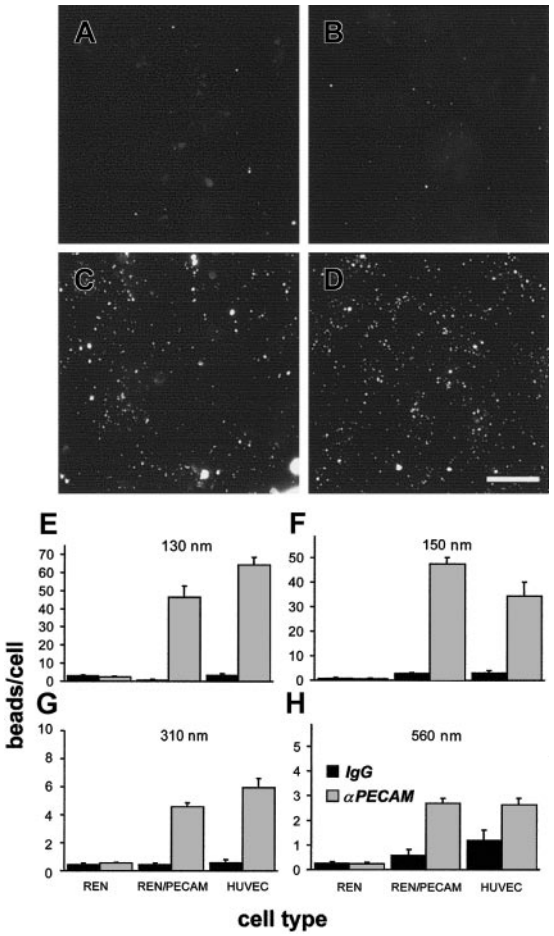

Figure 4. Anti-PECAM/beads bind to PECAM-expressing cells. (A-D) The 150-nm fluorescent beads coated with control IgG (A,B) or anti-PECAM (C,D) were incubated with REN/PECAM cells (A,C), or HUVECs (B,D) for 1 hour at 37°C, then washed, fixed, and imaged by fluorescence microscopy. Note the specific association of anti-PECAM/beads to PECAM-expressing cells (C,D). Bar, 10 μm. (E-H) Anti-PECAM/beads (light bars) or IgG/beads (dark bars) with effective diameters of 130 nm (E), 150 nm (F), 310 nm (G), or 560 nm (H) were incubated with REN cells, REN/PECAM cells, or HUVECs for 1 hour at 37°C. The cells were then washed, fixed, and analyzed by fluorescence microscopy. PECAM-expressing cell lines showed significantly more binding of anti-PECAM/beads than of IgG/beads ($P < .001$). There was little, if any, bead binding to nontransfected REN cells.

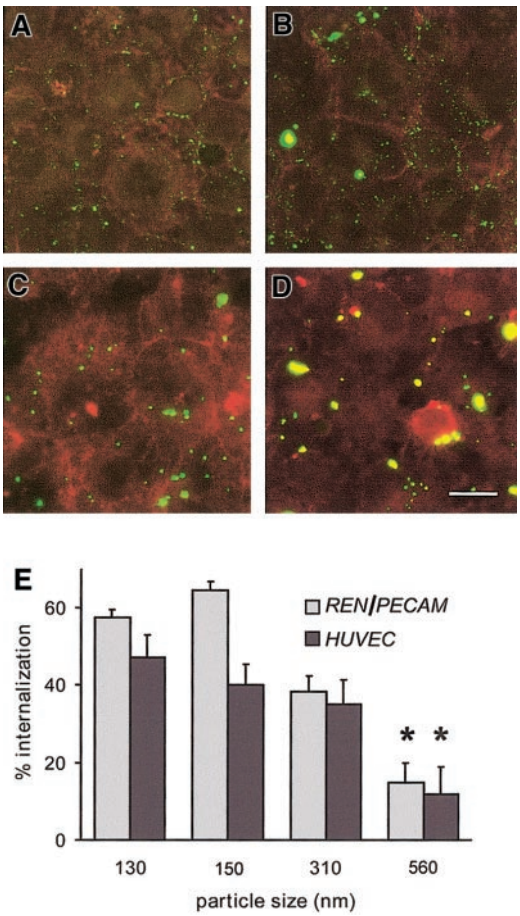

Figure 5. Size threshold for internalization of anti-PECAM/beads by REN/PECAM cells and HUVECs. (A-D) Anti-PECAM/beads with effective diameters of 130 nm (A), 150 nm (B), 310 nm (C), or 560 nm (D) were incubated with REN/PECAM cells for 1 hour at 37°C, washed, fixed, and counterstained with Texas Red–conjugated goat antimouse IgG without permeabilization. Thus, surface-bound beads appear yellow, while internalized beads appear green. Bar, 10 μm. (E) The internalized and surface-bound conjugate fractions of sized anti-PECAM/beads were determined in triplicate by image analysis. The percentage of internalized 560-nm beads was significantly lower than for smaller bead preparations (*$P < .05$).

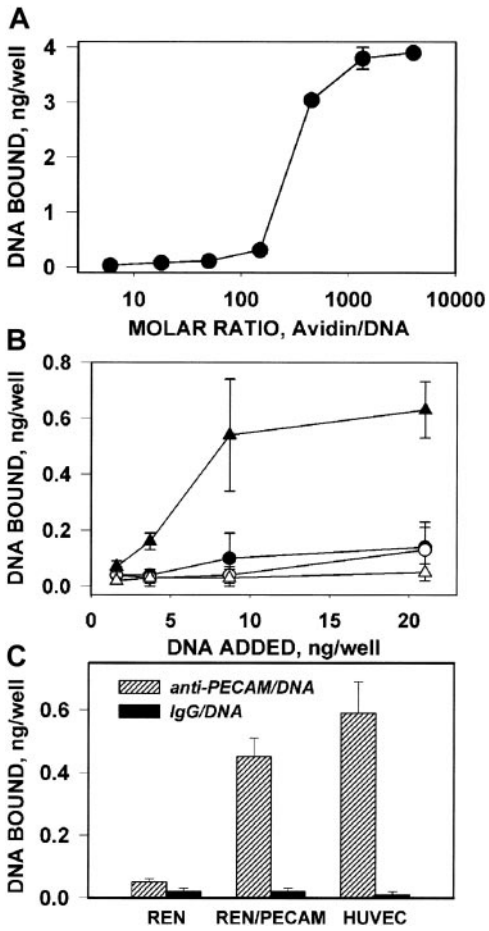

Figure 6. Antigen-binding properties of anti-PECAM/avidin/DNA complex. (A) Binding of ^{32}P-DNA/avidin complex, formed at various molar ratios, to plastic wells coated with biotinylated IgG. (B) Binding of anti-PECAM/avidin/^{32}P-DNA (triangles) and IgG/avidin/^{32}P-DNA (circles) complexes to plastic wells coated with recombinant PECAM (closed symbols) or albumin (open symbols). (C) Binding of anti-PECAM/avidin/^{32}P-DNA (hatched bars) and IgG/avidin/^{32}P-DNA (closed bars) complexes to wells with PECAM-expressing cells (REN/PECAMs and HUVECs) or control cells (REN). The data are shown as amount of ^{32}P-DNA bound per well, mean ± SD, n = 3.

gross lung injury index ALIS, small anti-PECAM/GOX caused markedly more severe lung injury than its larger counterpart.

Discussion

Both literature and intuition imply that the size of a carrier is an important parameter for targeting, internalization, and effects of a therapeutic cargo in drug and gene delivery strategies. Size affects cellular uptake and biodistribution of liposomes.[46-48] Polymerization and coupling to carriers enhance antibody internalization.[12,13,34] Both the charge and size of DNA/carrier complexes dictate the rate of their intracellular uptake, yet the results vary for different delivery systems and target cells.[35,36,49-51] The present study, focusing on immunotargeting to the constitutive endothelial antigens PECAMs and TM, shows that size control is critical for the design of optimal internalizable drug-delivery vehicles and thus provides a novel paradigm for intracellular vascular delivery of therapeutic cargoes.

We used SA-biotin and microbead techniques to produce conjugates of defined sizes and found that the conversion of poorly internalizable PECAM antibodies into effective carriers for the intracellular targeting of diverse cargoes required formation of multivalent anti-PECAM conjugates that were subject to a maximum size threshold. The uptake of anti-PECAM/SA and anti-PECAM/beads was significantly less efficient for complexes exceeding 350 nm in diameter. These data corroborate recent results that, with the use of radioisotope tracing and confocal and electron microscopy, show that anti-PECAM/SA carriers permit intracellular delivery of active enzymes to endothelial cells[30,45] and thus establish the optimal size parameters for the intracellular vascular immunotargeting of the conjugates.

The uptake of anti-PECAM conjugates differs from classical phagocytosis in macrophages and leukocytes, which internalize particles greater than a few microns in diameter. The 200- to 300-nm diameter of clathrin-coated pits[52] is consistent with the size threshold for anti-PECAM uptake. However, inhibitors of clathrin-mediated endocytosis do not prohibit anti-PECAM–mediated uptake (unpublished observation, May 1999), suggesting a different mechanism for the conjugates' internalization. However, inhibition of the uptake at 4°C excludes energy-independent mechanisms, such as the one apparently employed by some plasma membrane–permeating peptides (eg, TAT peptide of human immunodeficiency virus[53]).

It is also possible that the preferential uptake of particles smaller than 350 nm may be an intrinsic property of the cell types we examined (human endothelial and mesothelioma cells). For instance, the uptake of particles larger than 500 nm may require other specific signal transduction pathways that are present in the phagocytic cells but not in other cell types.[54] Consistent with this possibility, IgG-coated particles smaller than 1 μm internalized by macrophages are processed in a manner comparable to receptor-mediated endocytosis of soluble ligands, while larger particles are internalized by a phagocytic mechanism.[43] However, macrophages also partially internalize aggregated low-density lipoprotein and hydrophobic latex beads into surface-connected compartments

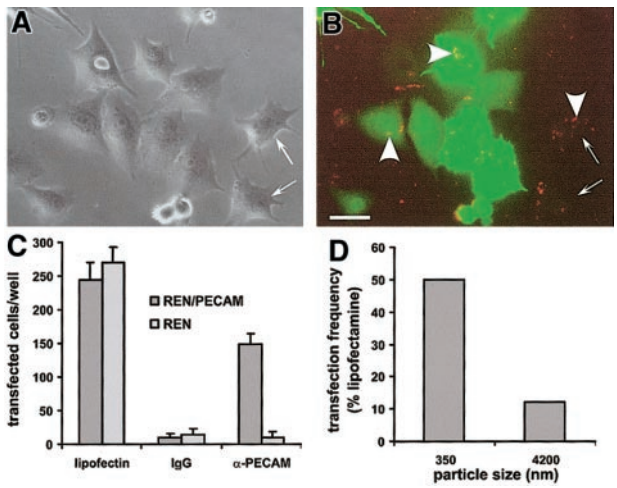

Figure 7. Transfection of REN/PECAM cells by rhodamine-labeled cDNA encoding GFP coupled with either anti-PECAM/SA-polylysine or IgG/SA-polylysine conjugates. (A) Phase-contrast image of REN/PECAM cells incubated with anti-PECAM/SA-polylysine/DNA polyplexes. The polyplexes' diameter was 350 nm. (B) Fluorescent image of the same field. The conjugate (arrowheads) bound to the PECAM-expressing cells and is visible as yellow and orange particles in the GFP-expressing (green) cells and red particles in cells lacking GFP expression. In spite of almost complete binding of anti-PECAM/SA-polylysine/DNA polyplexes, not all DNA-labeled cells expressed GFP (arrows). The polyplexes' diameter was 350 nm. (C) Transfection effectiveness of REN/PECAMs (dark bars) and control REN (light bars) cells by DNA/lipofectin (left), IgG/SA-polylysine/DNA (middle), and anti-PECAM/SA-polylysine/DNA complexes (right). The polyplexes' diameter was 350 nm. (D) Comparison of the transfection effectiveness of small (left) and large (right) anti-PECAM/SA-polylysine/DNA polyplexes in REN/PECAM cells.

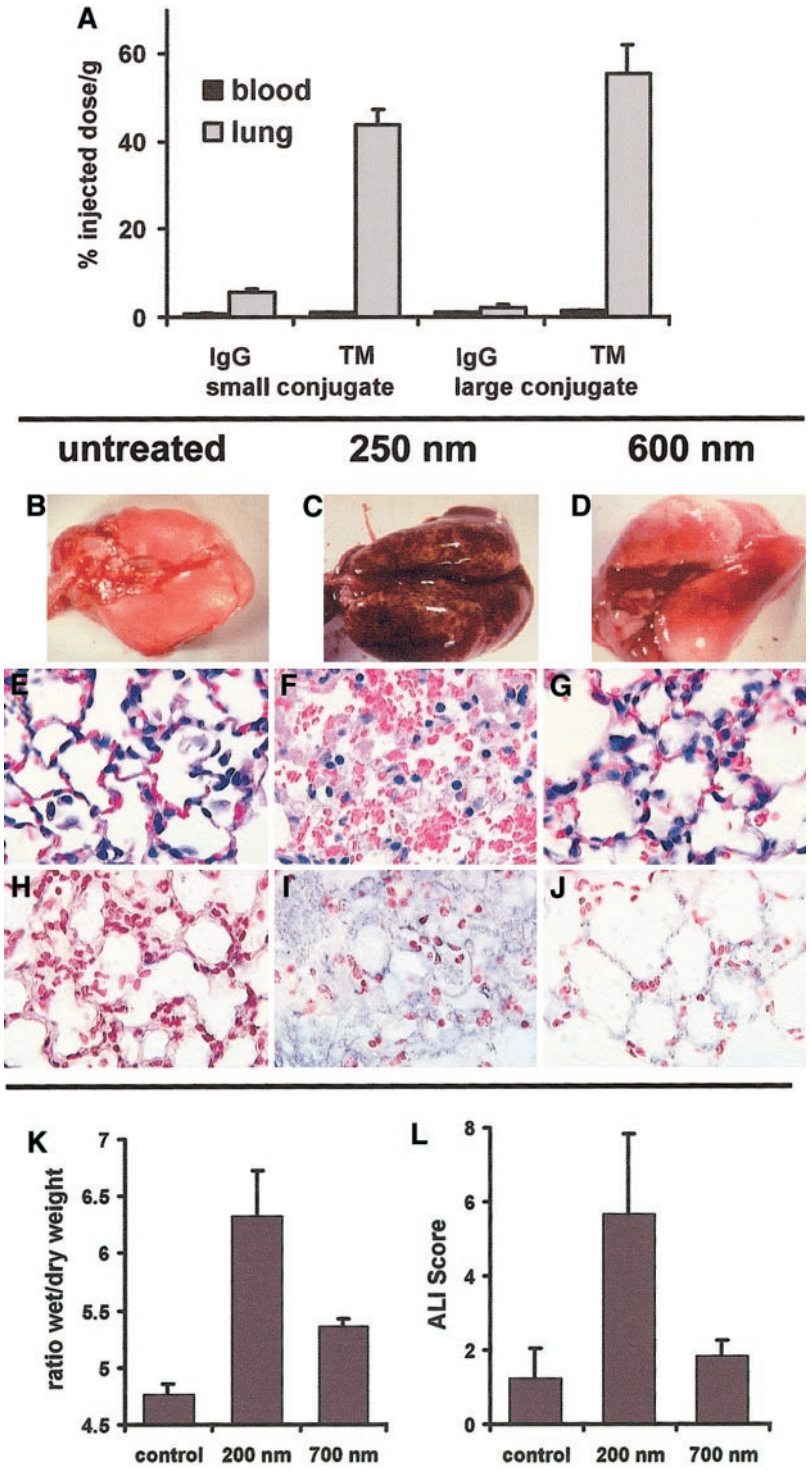

Figure 8. Effect of size on pulmonary targeting and effects of GOX conjugates (anti-PECAM/GOX and anti-TM/GOX) in intact mice. Blood level (black bars) and pulmonary uptake (gray bars) of small (250-nm, left part) versus large (600-nm, right part) anti-TM/^{125}I-GOX or IgG/^{125}I-GOX conjugates (2 to 3 μg per mouse) 1 hour after intravenous injection (panel A; accumulation data of anti-PECAM/^{125}I-GOX in murine lung are not shown). Pathological changes in the lungs harvested 3 hours after IV injection of 50 μg per mouse of small (C,F,I) or large (D,G,J) anti-TM/GOX conjugate versus saline injection (B,E,H). Panels B, C, and D show lung gross pathology; note severe hemorrhagic lung injury in panel C. Panels E, F, and G show hematoxylin/eosin staining of lung tissue sections; note edema and vascular injury in panel F. Panels H, I, and J show immunostaining for the products of lipid peroxidation; note positive reaction (blue color) in panel I. Original magnifications, panels E-J, × 40. Tissue edema determined as lung wet-to-dry ratio (K) and ALIS (L) in the lungs harvested 3 hours after IV injection of 50 μg per mouse of small (200-nm) or large (700-nm) anti-PECAM/GOX conjugate versus saline injection (control).

(patocytosis), which are subject to a 500-nm threshold.[55] It is conceivable that patocytosis and PECAM-mediated internalization may share some common mechanisms.[56]

There are also precedents for the internalization of large particles by cells other than professional phagocytes. For instance, fibroblasts transfected with receptors that mediate phagocytosis, such as the macrophage mannose receptor[57,58] and Fc receptors,[59-61] are capable of internalizing 1-μm particles, albeit at very low levels compared with macrophages and neutrophils.[62] Also, endothelial cells are subject to infection by internalized *Staphylococcus*,[63,64] *Candida*,[65] and *Listeria*,[66,67] all of which have a surface area greater than a 500-nm diameter particle. In these instances, though, a live infectious agent may play an active role in the internalization process.[67,68]

Results of recent studies from several groups imply that PECAM ligation may cause functional alterations in endothelial cells, although particular effects seem to be antibody-specific.[42,69,70] It is conceivable that intracellular targeting of conjugates internalized via PECAM may be influenced by receptor binding capacity and/or receptor clustering. For instance, monomeric versus polymeric complexes internalized by the Fc receptor are differentially recycled or targeted to lysosomes, respectively.[71,72] IgG complexes of 1 μm or larger are more efficiently

targeted to lysosomes than smaller complexes.[43] Oligomerized transferrin is internalized and retained in the recycling compartment,[73] while β–very low-density lipoprotein particles are targeted to either lysosomes or peripheral vesicles as they increase in size.[74] We are currently examining the intracellular targeting of anti-PECAM conjugates to determine whether particle size or receptor binding capacity determines the fate of these conjugates after internalization. This, in turn, should provide useful insights into the design of drug-delivery vehicles that optimize the lifetime of a conjugate-delivered enzyme activity or the effectiveness of DNA transduction.

Our finding that the threshold for effective intracellular delivery of DNA via PECAM-1 lies below 500 nm apparently contradicts the results of the recent study by Ross and Hui.[33] These authors studied the role of complex size in lipofectin-mediated intracellular delivery of DNA to Chinese hamster ovary cells and found that uptake and transfection increased gradually with increase in lipoplex size up to 2000 to 2500 nm.[33] This indicates that the mechanisms and size constraints for nontargeted uptake by fibroblasts that use lipoplexes differ from those of antigen-mediated targeted delivery of DNA to endothelium. For instance, interactions of lipoplexes, which can permeabilize the plasma membrane, may contribute to DNA uptake. Furthermore, the cellular events induced by targeted delivery of adenovirus directed to fibroblast growth factor receptor differ dramatically from those induced by a nontargeted virus.[75] Therefore, such parameters as cell type and status, as well as the nature of a target determinant and conjugate, should be carefully analyzed for every given delivery system.

Taken in the context of the vascular immunotargeting, our data establish the parameters for optimal intracellular drug delivery to endothelial cells. The facilitated uptake of 100- to 300-nm immunoconjugates provides a novel, powerful paradigm for intracellular vascular immunotargeting in vivo. Lung is a privileged vascular target that contains roughly a third of endothelium in the body and receives whole cardiac output of venous blood. Thus, antibodies directed against endothelial surface antigens (eg, anti-PECAM, anti-TM, and anti–angiotensin-converting enzyme) provide preferential pulmonary targeting, owing primarily to absolute perfusion and accessibility of pulmonary endothelium.[26-28,76] Recently, we have visualized intracellular uptake of reporter anti-PECAM/SA–β-gal conjugate by HUVECs in the pulmonary endothelium after injection in intact mice using confocal and electron microscopy,[30] but the significance of the conjugate size for the pulmonary targeting and effects has not been addressed.

In the present paper, we studied this issue, analyzing pulmonary immunotargeting of the H_2O_2-producing enzyme GOX in intact mice. We found previously that GOX conjugated with antiendothelial carriers, including anti-PECAM/SA, binds to and enters endothelial cells in cultures; generates H_2O_2 from glucose, thus killing the target cells[45]; and accumulates in the lungs after intravenous injection and causes acute pulmonary oxidative injury.[29,31] Importantly, studies in HUVECs revealed that GOX conjugated with internalizable antibodies causes more severe cellular injury than GOX associated with the cell surface, since intracellularly generated H_2O_2 is more toxic and less susceptible to extracellular antioxidants.[45,77]

In good agreement with in vitro findings, the small anti-PECAM/GOX and anti-TM/GOX conjugates caused markedly more severe oxidative vascular injury in murine lungs after intravenous injection than their large counterparts, despite similar uptake of the conjugates in the lungs (Figure 8). Therefore, the size of the GOX conjugates directed against 2 distinct endothelial antigens is critical for the local effect of the conjugated enzyme in the target organ in vivo. The most likely explanation for this result is that small internalizable GOX conjugates generate H_2O_2 intracellularly and thus produce more severe oxidative stress in the pulmonary endothelium, whereas H_2O_2 produced extracellularly by the large poorly internalizable counterparts associated with the vascular lumen is readily detoxified by blood antioxidants (eg, erythrocyte catalase and peroxidase). To our knowledge, this is the first direct demonstration of the role of the immunoconjugates' size on their targeting and effect in vivo.

In summary, the present results establish size-dependent endothelial uptake of affinity particles via poorly internalizable antigens. The results of pulmonary targeting of small and large GOX conjugates indicate that this paradigm operates in vivo and may therefore be useful for rational design and optimization of the subcellular addressing of cargoes to the target cells. For example, large poorly internalizable conjugates can be used to deliver and retain antithrombotic agents on the endothelium lumen, where they will be strategically positioned to intervene in coagulation and fibrinolysis. In contrast, small counterparts, even directed against the same surface determinants, can be used for delivery of genetic materials, antioxidant enzymes, and other cargoes requiring the intracellular addressing.

This study focused primarily on the endothelial cells, an important vascular target. However, size-dependent uptake of carriers may be a more general phenomenon. SA facilitates internalization of diverse monoclonal antibodies (eg, anti-PECAM, anti-TM) in distinct cell types (Table 1). Internalization of the conjugates prepared with antibodies to intercellular adhesion molecule-1 is subject to constraints similar to anti-PECAM conjugates in endothelial, mesothelial, and epithelial cells (unpublished observations, April 1999). Studies are underway to define the mechanisms that regulate the internalization of these conjugates and to determine whether this internalization pathway can be exploited for optimal intracellular immunotargeting of drugs in different cell types. Conceivably, size-controlled intracellular immunotargeting of toxic compounds (eg, GOX) to antigens expressed on tumor cells or tumor endothelium may eventually provide a new type of immunotoxin for tumor eradication.

Acknowledgments

We thank Dr M. Nakada (Centocor, Malvern, PA) for kindly supplying mAb 62; Dr A. Scherpereel and Mrs J. Argiris for help in animal experiments; and Drs D. Cines and T. D. Sweitzer for reading the manuscript and for valuable discussion.

References

1. Singh M. Transferrin as a targeting ligand for liposomes and anticancer drugs. Curr Pharm Des. 1999;5:443-451.
2. Nimni ME. Polypeptide growth factors: targeted delivery systems. Biomaterials. 1997;18:1201-1225.
3. Drapkin PT, O'Riordan CR, Yi SM, et al. Targeting the urokinase plasminogen activator receptor enhances gene transfer to human airway epithelia. J Clin Invest. 2000;105:589-596.
4. Muzykantov VR, Atochina EN, Ischiropoulos H, Danilov SM, Fisher AB. Immunotargeting of antioxidant enzyme to the pulmonary endothelium. Proc Natl Acad Sci U S A. 1996;93:5213-5218.
5. Atochina EN, Balyasnikova IV, Danilov SM, Granger DN, Fisher AB, Muzykantov VR. Immunotargeting of catalase to ACE or ICAM-1 protects perfused rat

lungs against oxidative stress. Am J Physiol. 1998; 275:L806–L817.

6. Poznansky MJ, Juliano RL. Biological approaches to the controlled delivery of drugs: a critical review. Pharmacol Rev. 1984;36:277-336.
7. Raso V. Immunotargeting intracellular compartments. Anal Biochem. 1994;222:297-304.
8. Muzykantov VR, Balyasnikova IV, Joshi A, et al. Epitope-dependent selective targeting of thrombomodulin monoclonal antibodies to either surface or intracellular compartment of endothelial cells. Drug Delivery. 1998;5:197-206.
9. Hurwitz E, Stancovski I, Sela M, Yarden Y. Suppression and promotion of tumor growth by monoclonal antibodies to ErbB-2 differentially correlate with cellular uptake. Proc Natl Acad Sci U S A. 1995;92:3353-3357.
10. Tagliabue E, Centis F, Campiglio M, et al. Selection of monoclonal antibodies which induce internalization and phosphorylation of p185HER2 and growth inhibition of cells with HER2/NEU gene amplification. Int J Cancer. 1991;47:933-937.
11. Better M, Bernhard SL, Fishwild DM, et al. Gelonin analogs with engineered cysteine residues form antibody immunoconjugates with unique properties. J Biol Chem. 1994;269:9644-9650.
12. Becerril B, Poul MA, Marks JD. Toward selection of internalizing antibodies from phage libraries. Biochem Biophys Res Commun. 1999;255:386-393.
13. Caron PC, Laird W, Co MS, Avdalovic NM, Queen C, Scheinberg DA. Engineered humanized dimeric forms of IgG are more effective antibodies. J Exp Med. 1992;176:1191-1195.
14. Muller WA, Weigl SA, Deng X, Phillips DM. PECAM-1 is required for transendothelial migration of leukocytes. J Exp Med. 1993;178:449-460.
15. Newman PJ. The biology of PECAM-1. J Clin Invest. 1997;100(suppl 11):S25–S29.
16. Yong KL, Watts M, Shaun Thomas N, Sullivan A, Ings S, Linch DC. Transmigration of CD34+ cells across specialized and nonspecialized endothelium requires prior activation by growth factors and is mediated by PECAM-1 (CD31). Blood. 1998;91:1196-1205.
17. Thompson RD, Noble KE, Larbi KY, et al. Platelet-endothelial cell adhesion molecule-1 (PECAM-1)-deficient mice demonstrate a transient and cytokine-specific role for PECAM-1 in leukocyte migration through the perivascular basement membrane. Blood. 2001;97:1854-1860.
18. Andre P, Denis CV, Ware J, et al. Platelets adhere to and translocate on von Willebrand factor presented by endothelium in stimulated veins. Blood. 2000;96:3322-3328.
19. Esmon CT. Thrombomodulin as a model of molecular mechanisms that modulate protease specificity and function at the vessel surface. FASEB J. 1995;9:946-955.
20. Cramer EM, Berger G, Berndt MC. Platelet alpha-granule and plasma membrane share two new components: CD9 and PECAM-1. Blood. 1994; 84:1722-1730.
21. Zehnder JL, Shatsky M, Leung LL, Butcher EC, McGregor JL, Levitt LJ. Involvement of CD31 in lymphocyte-mediated immune responses: importance of the membrane-proximal immunoglobulin domain and identification of an inhibiting CD31 peptide. Blood. 1995;85:1282-1288.
22. Patil S, Newman DK, Newman PJ. Platelet endothelial cell adhesion molecule-1 serves as an inhibitory receptor that modulates platelet responses to collagen. Blood. 2001;97:1727-1732.
23. Vaporciyan AA, DeLisser HM, Yan HC, et al. Involvement of platelet-endothelial cell adhesion molecule-1 in neutrophil recruitment in vivo. Science. 1993;262:1580-1582.
24. Murohara T, Delyani JA, Albelda SM, Lefer AM. Blockade of platelet endothelial cell adhesion molecule-1 protects against myocardial ischemia and reperfusion injury in cats. J Immunol. 1996; 156:3550-3557.
25. Gumina RJ, el Schultz J, Yao Z, et al. Antibody to platelet/endothelial cell adhesion molecule-1 reduces myocardial infarct size in a rat model of ischemia-reperfusion injury. Circulation. 1996;94: 3327-3333.
26. Ford VA, Stringer C, Kennel SJ. Thrombomodulin is preferentially expressed in Balb/c lung microvessels. J Biol Chem. 1992;267:5446-5450.
27. Maruyama K, Kennel SJ, Huang L. Lipid composition is important for highly efficient target binding and retention of immunoliposomes. Proc Natl Acad Sci U S A. 1990;87:5744-5748.
28. Muzykantov VR, Christofidou-Solomidou M, Balyasnikova I, et al. Streptavidin facilitates internalization and pulmonary targeting of an anti-endothelial cell antibody (platelet-endothelial cell adhesion molecule 1): a strategy for vascular immunotargeting of drugs. Proc Natl Acad Sci U S A. 1999;96:2379-2384.
29. Christofidou-Solomidou M, Pietra GG, Solomides CC, et al. Immunotargeting of glucose oxidase to endothelium in vivo causes oxidative vascular injury in the lungs. Am J Physiol Lung Cell Mol Physiol. 2000;278:L794–L805.
30. Scherpereel A, Wiewrodt R, Christofidou-Solomidou M, et al. Cell-selective intracellular delivery of a foreign enzyme to endothelium in vivo using vascular immunotargeting. FASEB J. 2001;15: 416-426.
31. Christofidou-Solomidou M, Ng K, Kennel S, Pietra G, Muzykantov V, Albelda S. Immunotargeting of glucose oxidase to thrombomodulin causes ARDS-like oxidative lung injury in mice. Am J Respir Crit Care Med. 1999;159:A890.
32. Li S, Tan Y, Viroonchatapan E, Pitt BR, Huang L. Targeted gene delivery to pulmonary endothelium by anti-PECAM antibody. Am J Physiol Lung Cell Mol Physiol. 2000;278:L504–L511.
33. Ross PC, Hui SW. Lipoplex size is a major determinant of in vitro lipofection efficiency. Gene Ther. 1999;6:651-659.
34. Nielsen UB, Marks JD. Internalizing antibodies and targeted cancer therapy: direct selection from phage display libraries. Pharm Sci Technol Today. 2000;3:282-291.
35. Schaffer DV, Lauffenburger DA. Optimization of cell surface binding enhances efficiency and specificity of molecular conjugate gene delivery. J Biol Chem. 1998;273:28004-28009.
36. Xu B, Wiehle S, Roth JA, Cristiano RJ. The contribution of poly-L-lysine, epidermal growth factor and streptavidin to EGF/PLL/DNA polyplex formation. Gene Ther. 1998;5:1235-1243.
37. Brown EJ. Phagocytosis [review]. Bioessays. 1995;17:109-117.
38. Allen LA, Aderem A. Mechanisms of phagocytosis [review]. Curr Opin Immunol. 1996;8:36-40.
39. Kwiatkowska K, Sobota A. Signaling pathways in phagocytosis. Bioessays. 1999;21:422-431.
40. Yan HC, Pilewski JM, Zhang Q, DeLisser HM, Romer L, Albelda SM. Localization of multiple functional domains on human PECAM-1 (CD31) by monoclonal antibody epitope mapping. Cell Adhes Commun. 1995;3:45-66.
41. Smythe WR, Kaiser LR, Hwang HC, et al. Successful adenovirus-mediated gene transfer in an in vivo model of human malignant mesothelioma [comment appears in Ann Thorac Surg. 1994;57: 1383-1384]. Ann Thorac Surg. 1994;57:1395-1401.
42. Gurubhagavatula I, Amrani Y, Pratico D, Ruberg FL, Albelda SM, Panettieri RA Jr. Engagement of human PECAM-1 (CD31) on human endothelial cells increases intracellular calcium ion concentration and stimulates prostacyclin release. J Clin Invest. 1998;101:212-222.
43. Koval M, Preiter K, Adles C, Stahl PD, Steinberg TH. Size of IgG-opsonized particles determines macrophage response during internalization. Exp Cell Res. 1998;242:265-273.
44. Berne BJ, Pecora R. Dynamic Light Scattering with Applications to Chemistry, Biology and Physics. Malabar, FL: Robert E. Krieger, 1990.
45. Gow AJ, Branco F, Christofidou-Solomidou M, Black-Schultz L, Albelda SM, Muzykantov VR. Immunotargeting of glucose oxidase: intracellular production of H_2O_2 and endothelial oxidative stress. Am J Physiol. 1999;277:L271–L281.
46. Torchilin VP. Affinity liposomes in vivo: factors influencing target accumulation. J Mol Recognit. 1996;9:335-346.
47. Kulkarni SB, Betageri GV, Singh M. Factors affecting microencapsulation of drugs in liposomes. J Microencapsul. 1995;12:229-246.
48. Jones MN. The surface properties of phospholipid liposome systems and their characterisation. Adv Colloid Interface Sci. 1995;54:93-128.
49. Garnett MC. Gene-delivery systems using cationic polymers. Crit Rev Ther Drug Carrier Syst. 1999;16:147-207.
50. Luo D, Saltzman WM. Synthetic DNA delivery systems. Nat Biotechnol. 2000;18:33-37.
51. Turek J, Dubertret C, Jaslin G, Antonakis K, Scherman D, Pitard B. Formulations which increase the size of lipoplexes prevent serum-associated inhibition of transfection. J Gene Med. 2000;2:32-40.
52. Mukherjee S, Ghosh RN, Maxfield FR. Endocytosis [review]. Physiol Rev. 1997;77:759-803.
53. Schwarze SR, Ho A, Vocero-Akbani A, Dowdy SF. In vivo protein transduction: delivery of a biologically active protein into the mouse [comment appears in Science. 1999;285:1466-1467]. Science. 1999;285:1569-1572.
54. Cox D, Tseng CC, Bjekic G, Greenberg S. A requirement for phosphatidylinositol 3-kinase in pseudopod extension. J Biol Chem. 1999;274: 1240-1247.
55. Kruth HS, Chang J, Ifrim I, Zhang WY. Characterization of patocytosis: endocytosis into macrophage surface-connected compartments. Eur J Cell Biol. 1999;78:91-99.
56. Kruth HS, Zhang WY, Skarlatos SI, Chao FF. Apolipoprotein B stimulates formation of monocyte-macrophage surface-connected compartments and mediates uptake of low density lipoprotein-derived liposomes into these compartments. J Biol Chem. 1999;274:7495-7500.
57. Kruskal BA, Sastry K, Warner AB, Mathieu CE, Ezekowitz RA. Phagocytic chimeric receptors require both transmembrane and cytoplasmic domains from the mannose receptor. J Exp Med. 1992;176:1673-1680.
58. Ezekowitz RA, Sastry K, Bailly P, Warner A. Molecular characterization of the human macrophage mannose receptor: demonstration of multiple carbohydrate recognition-like domains and phagocytosis of yeasts in Cos-1 cells. J Exp Med. 1990;172:1785-1794.
59. Indik Z, Kelly C, Chien P, Levinson AI, Schreiber AD. Human Fc gamma RII, in the absence of other Fc gamma receptors, mediates a phagocytic signal. J Clin Invest. 1991;88:1766-1771.
60. Joiner KA, Fuhrman SA, Miettinen HM, Kasper LH, Mellman I. Toxoplasma gondii: fusion competence of parasitophorous vacuoles in Fc receptor-transfected fibroblasts. Science. 1990;249:641-646.
61. Odin JA, Edberg JC, Painter CJ, Kimberly RP, Unkeless JC. Regulation of phagocytosis and [Ca2+]i flux by distinct regions of an Fc receptor. Science. 1991;254:1785-1788.
62. Brown EJ, Steinberg TH. Phagocytosis [review]. Biomembranes. 1996;4:33-63.
63. Menzies BE, Kourteva I. Internalization of Staphylococcus aureus by endothelial cells induces apoptosis. Infect Immun. 1998;66:5994-5998.

64. Yao L, Bengualid V, Lowy FD, Gibbons JJ, Hatcher VB, Berman JW. Internalization of Staphylococcus aureus by endothelial cells induces cytokine gene expression. Infect Immun. 1995;63:1835-1839.
65. Filler SG, Swerdloff JN, Hobbs C, Luckett PM. Penetration and damage of endothelial cells by Candida albicans. Infect Immun. 1995;63:976-983.
66. Greiffenberg L, Goebel W, Kim KS, et al. Interaction of Listeria monocytogenes with human brain microvascular endothelial cells: InlB-dependent invasion, long-term intracellular growth, and spread from macrophages to endothelial cells. Infect Immun. 1998;66:5260-5267.
67. Drevets DA. Listeria monocytogenes virulence factors that stimulate endothelial cells. Infect Immun. 1998;66:232-238.
68. Alvarez-Dominguez C, Barbieri AM, Beron W, Wandinger-Ness A, Stahl PD. Phagocytosed live Listeria monocytogenes influences Rab5-regulated in vitro phagosome-endosome fusion. J Biol Chem. 1996;271:13834-13843.
69. Yang S, Graham J, Kahn JW, Schwartz EA, Gerritsen ME. Functional roles for PECAM-1 (CD31) and VE-cadherin (CD144) in tube assembly and lumen formation in three-dimensional collagen gels. Am J Pathol. 1999;155:887-895.
70. Chiba R, Nakagawa N, Kurasawa K, Tanaka Y, Saito Y, Iwamoto I. Ligation of CD31 (PECAM-1) on endothelial cells increases adhesive function of alphavbeta3 integrin and enhances beta1 integrin-mediated adhesion of eosinophils to endothelial cells. Blood. 1999;94:1319-1329.
71. Mellman I, Plutner H. Internalization and degradation of macrophage Fc receptors bound to polyvalent immune complexes. J Cell Biol. 1984; 98:1170-1177.
72. Mellman I, Plutner H, Ukkonen P. Internalization and rapid recycling of macrophage Fc receptors tagged with monovalent antireceptor antibody: possible role of a prelysosomal compartment. J Cell Biol. 1984;98:1163-1169.
73. Marsh EW, Leopold PL, Jones NL, Maxfield FR. Oligomerized transferrin receptors are selectively retained by a lumenal sorting signal in a long-lived endocytic recycling compartment. J Cell Biol. 1995;129:1509-1522.
74. Tabas I, Myers JN, Innerarity TL, et al. The influence of particle size and multiple apoprotein E-receptor interactions on the endocytic targeting of beta-VLDL in mouse peritoneal macrophages. J Cell Biol. 1991;115:1547-1560.
75. Doukas J, Hoganson DK, Ong M, et al. Retargeted delivery of adenoviral vectors through fibroblast growth factor receptors involves unique cellular pathways. FASEB J. 1999;13: 1459-1466.
76. Muzykantov VR, Danilov SM. Glucose oxidase conjugated with anti-endothelial monoclonal antibodies: in vitro and in vivo studies. Int J Radiat Biol. 1991;60:11-15.
77. Muzykantov VR, Trubetskaya OV, Puchnina EA, Sakharov DV, Domogatsky SP. Cytotoxicity of glucose oxidase conjugated with antibodies to target cells: killing efficiency depends on the conjugate internalization. Biochim Biophys Acta. 1990;1053:27-31.